Horsehair worm infection reshapes host trait architecture via allometric and sex-specific allocation shifts

Shotaro Tani[1,2], Keito Tsunoda[2], Asami Kajimoto[2,3], Koichiro Kawai[2], Kenji Toyota[2,3,4*]

[1]Center for Ecological Research, Kyoto University, 2-509-3 Hirano Otsu, Shiga 520-2113, Japan.
[2]Department of Bioresource Science, Graduate School of Integrated Sciences for Life, Hiroshima University, 1-4-4 Kagamiyama, Higashihiroshima-shi, Hiroshima 739-8528, Japan.
[3]Department of Biological Sciences, Faculty of Science, Kanagawa University, 3-27-1, Rokkakubashi, Kanagawa-ku, Yokohama-city, Kanagawa, 221-8686, Japan.
[4]Department of Biological Science and Technology, Faculty of Industrial Science and Technology, Tokyo University of Science, 6-3-1 Niijuku, Katsushika-ku, Tokyo, 125-8585, Japan.

[*]Correspondence to:
Dr. Kenji Toyota: toyotak@hiroshima-u.ac.jp

Abstract

1. Parasites can profoundly modify host phenotype, yet most studies emphasize behavioral manipulation rather than changes in morphology. From a functional perspective, organismal performance depends on proportional investment among traits, suggesting that parasitism may alter trait architecture through changes in allometry rather than simply reducing body size.
2. Here we test whether infection by *Chordodes* horsehair worms (Nematomorpha) reorganizes host morphology in two mantis species. Using multivariate analyses (PERMANOVA) and allometric models (ANCOVA), we quantified how infection affects scaling relationships, sexual dimorphism and multivariate trait structure occupancy.
3. Infection altered proportional changes among traits rather than causing uniform shrinkage. In the Chinese mantis *Tenodera sinensis*, thoracic and wing traits showed reduced scaling and sexual dimorphism contracted, whereas in the giant Asian mantis *Hierodula patellifera*, appendage traits were primarily affected, and dimorphism was amplified or reversed. Thus, parasite effects were sex-specific and species-dependent.
4. These patterns closely parallel parasite-induced feminization and trait reallocation documented in rhizocephalan–crab systems, suggesting a general mechanism whereby parasites redirect developmental investment.
5. Our results demonstrate that parasites reorganize functional morphology through allometric reallocation, thereby modifying performance-related traits and potentially altering evolutionary trajectories. Integrating parasitism into trait-based ecology is therefore essential for understanding how organismal form, function and diversification are linked.

Keywords

allometry, functional traits, host–parasite interactions, parasite manipulation, sexual dimorphism,

Plain Language Summary

Parasites do not simply shrink their hosts — they can fundamentally redesign them. We found that horsehair worms (a type of parasite that lives inside praying mantises) alter the proportions of the host body in ways far beyond simple size reduction. The wings, thorax, and legs of infected mantises scale differently relative to body size compared to uninfected ones, and these changes differ between male and female hosts and between the two mantis species studied. Our results suggest that parasites can act as architects of host body shape, with potential consequences for how infected animals move, reproduce, and interact with their environment.

Introduction

Parasites are increasingly recognized as powerful drivers of host phenotype, modifying behavior, physiology and morphology in ways that ultimately influence ecological performance and ecosystem processes. Beyond direct pathological costs, parasites can reshape functional traits that determine locomotion, dispersal and reproduction, thereby altering how organisms interact with their environments and food webs. Striking examples come from horsehair worms (phylum Nematomorpha), whose manipulation of terrestrial arthropod hosts can redirect energy flow from land to freshwater systems, effectively restructuring ecosystem linkages (Sato et al., 2011; Sato et al., 2012). These findings have reframed parasites as ecological engineers rather than passive consumers.

Research on horsehair worms has primarily focused on behavioral manipulation. Infected mantises are induced to enter water, a striking example of extended parasite phenotype (Thomas et al., 2002). Recent mechanistic work has demonstrated that this behavior is mediated by altered sensory responses, including enhanced polarotaxis toward horizontally polarized light reflected from water surfaces (Obayashi et al., 2021), and parasite-derived gene expression and horizontally transferred genes that may modulate host neural pathways (Mishina et al., 2023). Furthermore, anthropogenic environments can interact with this manipulation, generating ecological traps that alter parasite transmission dynamics (Sawada et al., 2024). Together, these studies illustrate how horsehair worms modify host behavior to influence ecological processes. However, whether infection also reorganizes host morphology and functional trait architecture remains largely unexplored, with only one study (Chiu et al., 2015) demonstrating that infection alters host functional morphology.

From a functional perspective, organismal performance depends not only on absolute body size but on proportional investment among traits. Allometric scaling relationships determine mechanical leverage, locomotor efficiency and reproductive allocation, meaning that shifts in proportional growth can have larger ecological consequences than simple reductions in condition. Trait-based ecology therefore predicts that processes diverting energy or development—such as parasitism—should alter scaling relationships and multivariate trait combinations rather than uniformly depress growth (West et al., 1997; Violle et al., 2007; Hatcher et al., 2012).

Another consideration is that male and female phenotypes of organisms often diverge

as sexual dimorphism due to sex-specific allocation strategies shaped by fecundity and sexual selection. Because these traits are energetically costly, parasitism may differentially affect investment in male-versus-female-biased structures, leading to reductions, exaggerations or reversals of dimorphism. Thus, sexual dimorphism provides a particularly sensitive framework for detecting parasite-induced changes. Indeed, sex-biased impacts of parasitism are widely reported across taxa and linked to hormonal and immunological differences between sexes (Zuk & McKean, 1996; Klein, 2004).

Importantly, parasite effects may also depend on host–parasite compatibility and host range. Even closely related horsehair worm species differ in the breadth of hosts they infect and in their physiological interactions with mantids, suggesting that parasite identity shapes infection outcomes (Tani et al., 2024). Such differences imply that morphological consequences of infection may be species-contingent rather than universal. Comparative analyses across host species are therefore necessary to distinguish general mechanisms from context-dependent effects. However, few studies have quantified or compared how infection by each parasite species alters the structural expression of sexually dimorphic morphology in each host species.

Here, we test whether infection by horsehair worms reorganizes host functional morphology through changes in allometric scaling and multivariate trait architecture rather than simple body-size reduction. Using two mantis species, we integrate ANCOVA to quantify changes in trait–size relationships and PERMANOVA to detect shifts in multivariate trait structure. We predict that infection (i) alters allometric slopes of locomotor and thoracic traits, (ii) modifies sexual dimorphism through sex-specific allocation shifts, and (iii) produces species-dependent responses reflecting host–parasite compatibility. By framing parasitism within a trait-based and allometric context, we evaluate parasites as drivers of functional morphology and potential agents of evolutionary diversification.

Materials and Methods

Study system and sampling

We investigated morphological consequences of infection by horsehair worms in two mantis species: *Tenodera sinensis* Saussure, 1871 and *Hierodula patellifera* Serville, 1839, which

commonly serve as definitive terrestrial hosts for *Chordodes japonensis* Inoue, 1951 and *C. formosanus* Chiu, 2011, respectively (Tani et al., 2024). Both species are widespread generalist predators and exhibit marked sexual dimorphism in body proportions. Adult mantises were collected sequentially between October 12, 2018 and September 27, 2023, in Hachihonmatsu, Kochi, Kagamiyama, Saijo and Takaya, Higashihiroshima City, Hiroshima Prefecture. Individuals were captured by hand or sweep net and immediately transported to the laboratory. For each specimen, species and sex were determined based on body shape and external genital morphology referring to Nakamine (2016). Infection status was assessed by submerging in water to encourage the parasites to emerge or by dissection of the abdominal cavity after euthanasia; individuals containing one or more horsehair worms were classified as infected, whereas those lacking parasites with developed gonads were classified as uninfected. Individuals were therefore assigned to four groups per species: female–uninfected, female–infected, male–uninfected, and male–infected. Note that the infected mantis samples from 2018 to 2021 were the same as those used in Tani et al. (2024).

Parasite identification

We determined the species of hairworms by DNA barcoding. The method used was the same as in Tani et al. (2024), as follows. A partial sequence within the mitochondrial CO1 gene was amplified by PCR with the universal primers, LCO1490 and HCO2198 (Folmer et al., 1994) or designed specific primers, ChCO1F and ChCO1R for amplifying shorter fragment (458 bp). Each amplified fragment was sequenced by Sanger sequencing at Eurofins Genomics K.K. (Tokyo, Japan). Sequence data were integrated and aligned using MEGA for Mac OS (Stecher et al., 2020), and each sequence was assigned to species (*C. japonensis* or *C. formosanus*) based on its position on the neighbor-joining phylogenetic tree. All determined sequences have been deposited in GenBank along with their collection information (see Table S1 and S2).

Morphological measurements

To quantify functional morphology, we measured pronotum length (PL) as a proxy for body size and 16 additional linear traits representing thoracic, wing and locomotor-appendage structures (see Fig. 1). Following Chiu et al. (2015), we did not use overall body length as a

proxy of body size, for the abdomen is telescopic and therefore unsuitable as a body-size proxy. Traits included pronotum width (PW), forewing length (FWL) and width (FWW), hindwing length (HWL), and lengths of fore-leg (FLL), fore-coxa (FLCX), fore-femur (FLFM) and fore-tibia (FLTB), lengths of mid-leg (MLL), mid-coxa (MLCX), mid-femur (MLFM) and mid-tibia (MLTB), and lengths of hind-leg (HLL), hind-coxa (HLCX), hind-femur (HLFM) and hind-tibia (HLTB). The measurement locations for all traits were standardized according to Brannoch et al. (2017). Measurements were taken by a digital caliper CD-S15C (Mitutoyo, Japan) to the nearest 0.01 mm. Each individual was positioned dorsally and laterally to ensure consistent landmark placement. All measurements were performed by a single observer to minimize measurement error. PL was used as the independent size variable for all allometric analyses.

Replication statement

Scale of inference	Scale at which factor of interest is applied	Number of replicates at the appropriate scale
Individuals (within *T. sinensis*)	Individual	17 infected, 22 uninfected
Individuals (within *H. patellifera*)	Individual	23 infected, 30 uninfected

Statistical framework

Analyses were conducted separately for each species to evaluate species-specific responses to infection. All analyses were performed in R version 4.5.2 (R Core Team, 2025). We adopted a trait-based and allometric framework to test whether infection altered proportional allocation among traits rather than simply reducing body size.

Multivariate trait structure

To evaluate whether infection, sex and body size influenced overall morphology, we analyzed the multivariate trait matrix using permutational multivariate analysis of variance (PERMANOVA). Euclidean distances were calculated from standardized trait values. Models included parasite status (PR), host sex (HSX) and PL as predictors:

$$\text{trait matrix} \sim PR + HSX + PL$$

Permutation tests (999 permutations) were conducted using the adonis2 function in the R package 'vegan' (version 2.7.2). We report pseudo-F statistics, R^2 values and permutation-based P-values. This analysis tests whether infection shifts individuals in multivariate trait space independently of body size.

Allometric analyses of individual traits

To quantify trait-specific scaling relationships, we fitted analysis of covariance (ANCOVA) models for each morphological trait:

$$\text{trait} \sim PL + PR + HSX + PR \times HSX$$

where PL represents body size, PR parasite status, and HSX sex. Significant PR or PR × HSX effects indicate parasite-mediated changes in allometric intercepts or slopes. For each model we extracted regression coefficients, standard errors, and P-values. Model assumptions were checked by visual inspection of residuals.

Sexual dimorphism and estimated marginal means

To compare trait values among sex × parasite groups at equivalent body size, we calculated estimated marginal means (EMMs) from ANCOVA models using the R package 'emmeans' (version 2.0.1). Pairwise contrasts were used to quantify:

1. sexual dimorphism in uninfected individuals
2. parasite effects within each sex
3. sexual dimorphism in infected individuals

Effect sizes are reported as estimated differences ± SE.

Visualization and software

Allometric relationships were visualized using scatterplots of trait values against pronotum length with group-specific linear regressions (sex × parasite). Multivariate patterns were summarized using ordination plots and model summaries. All statistical analyses were

conducted in R using packages ‘vegan’, ‘car’, ‘broom’, ‘emmeans’. Code is available upon request to ensure reproducibility.

Results

Multivariate morphological structure

Across both mantis species, body proportions differed systematically with sex and, to a lesser extent, parasite infection. Multivariate analyses (PERMANOVA) revealed that overall morphology was strongly structured by sex and body size in both species, with additional parasite effects that varied between hosts. In *T. sinensis*, parasite infection significantly influenced multivariate morphology (pseudo-F = 4.218, P = 0.027), alongside strong effects of host sex (pseudo-F = 17.703, P = 0.001) and host body size (pseudo-F = 45.151, P = 0.001). Sex explained a larger proportion of variation (R^2 = 0.151) than infection alone (R^2 = 0.036), indicating pronounced baseline sexual dimorphism with superimposed parasite effects. In contrast, *H. patellifera* showed strong effects of host sex (pseudo-F = 10.376, P = 0.001) and host body size (pseudo-F = 78.583, P = 0.001), whereas parasite status did not significantly alter multivariate trait space (pseudo-F = 1.384, P = 0.248). Thus, infection effects in this species were subtle at the whole-body level and emerged primarily at the level of individual traits.

Trait–size scaling and allometric shifts

Despite strong overall size dependence, infection frequently altered proportional trait allocation rather than causing uniform size reduction. Scatterplots of trait values against pronotum length (PL) revealed consistent linear scaling for all measurements, but regression slopes and intercepts diverged among sex × parasite categories (Fig. 2 for *T. sinensis* and Fig. 3 for *H. patellifera*). ANCOVA analyses confirmed widespread allometric responses (Table 1 for *T. sinensis* and Table 2 for *H. patellifera*). Several traits exhibited significant parasite or sex × parasite effects, demonstrating that infection modified trait scaling relative to body size. In *T. sinensis*, thoracic and wing-related traits showed the strongest responses. Infected females exhibited reduced pronotum width relative to size, while infected males showed shorter forewings and altered femur proportions. Multiple traits displayed significant

interaction terms, indicating that proportional investment shifted differently between sexes. In *H. patellifera*, parasite effects were concentrated in locomotor appendages. Mid- and hind-leg femora and tibiae showed reduced scaling in infected males, whereas females showed weaker or opposite responses. These patterns indicate selective modification of appendage architecture rather than generalized shrinkage.

Parasite effects on sexual dimorphism

Parasite infection consistently modified the magnitude and direction of sexual dimorphism, but the direction of change differed between species **(Table 3 for *T. sinensis* and Table 4 for *H. patellifera*)**. In *T. sinensis*, several traits that were strongly sexually dimorphic under uninfected conditions showed reduced differences after infection. For example, females normally had wider pronota than males, but this gap decreased when infected, indicating contraction of sexual dimorphism. Wing and thoracic measurements similarly showed reduced intersexual separation. In contrast, *H. patellifera* exhibited the opposite pattern for several appendage traits. Under uninfected conditions, some traits showed little sexual difference, yet infection generated clear divergence, with males becoming shorter and females longer (e.g., MLTB). Thus, infection amplified or reversed dimorphism in this species. These contrasting responses indicate that parasite effects are sex-specific and cannot be explained by general body-size reduction.

Species-specific responses to infection

Direct comparison of the two species revealed qualitatively different morphological consequences of parasitism. In *T. sinensis*, infection primarily altered thoracic and wing structures and tended to compress sexual dimorphism. In *H. patellifera*, infection predominantly affected appendage lengths and often enhanced or reversed dimorphism. These contrasting multivariate trait structure displacements suggest that parasite impacts depend strongly on host-specific developmental or functional architecture rather than reflecting a universal response to infection.

Summary of patterns

Across both species, parasite infection did not simply reduce overall size. Instead, infection reshaped host morphology by modifying allometric relationships, selectively reallocating investment among functional traits, and producing sex-dependent and species-specific shifts in trait architecture. Together, these results demonstrate that parasitism reorganizes host functional morphology rather than acting as a uniform physiological stressor.

Discussion

Parasites reorganize host body plans through allometric reallocation rather than generalized shrinkage

Our results demonstrate that horsehair worm infection does not simply reduce host body size but instead restructures proportional investment among traits, thereby altering allometric relationships and shifting individuals within multivariate trait space. Such patterns indicate developmental or physiological reallocation rather than condition-dependent shrinkage, consistent with the view that organismal performance is governed by trait proportions rather than absolute size (West et al., 1997). From a functional-trait perspective, proportional architecture determines mechanical leverage, locomotor efficiency and energetic allocation, meaning that changes in scaling relationships can have disproportionate ecological consequences (Violle et al., 2007). Parasitism therefore represents a mechanism capable of reorganizing host trait architecture, rather than acting solely as a generalized stressor (Hatcher et al., 2012; Lafferty & Shaw, 2013).

Species contingency and host–parasite compatibility

Although trait reorganization emerged as a common outcome, the magnitude and direction of parasite effects differed markedly between host species. Whole-body multivariate trait shifts were pronounced in *T. sinensis* but weaker in *H. patellifera*, and the traits most affected differed between species. Such contingency likely reflects host-specific developmental architecture and physiological compatibility with parasites (Poulin, 2010). Differences among horsehair worm species in host range and infection dynamics further suggest that parasite identity shapes phenotypic outcomes (Tani et al., 2024). Parasite-induced morphological change should therefore be viewed as a context-dependent process constrained by host–

parasite compatibility rather than a uniform response to infection (Hatcher et al., 2012; Poulin, 2010).

Functional consequences for performance and ecosystem processes

The traits most affected by infection—thoracic dimensions, wings and appendages—are directly linked to locomotion, dispersal and mating behavior, suggesting that allometric modification is likely to influence performance and ecological interactions. As previously mentioned, horsehair worms are well known for manipulating host behavior to induce water entry, thereby transferring terrestrial biomass into aquatic ecosystems (Sato et al., 2011; Sato et al., 2012), and such manipulation has been shown to be mediated by altered sensory processing, including enhanced polarotaxis toward horizontally polarized light (Obayashi et al., 2021). Our findings suggest that morphological modification may act in concert with behavioral manipulation, jointly shaping how infected hosts move through landscapes and interact with food webs (Thomas et al., 2002; Sato et al., 2012).

Sex-specific trait reallocation and restructuring of sexual dimorphism

Parasite infection consistently altered the magnitude and direction of sexual dimorphism, although the direction of change differed between host species. Sexually dimorphic traits often represent energetically costly investments shaped by fecundity selection and sexual selection, making them particularly sensitive to parasite-induced resource diversion (Shine, 1989; Zuk & McKean, 1996). Parasite interference with endocrine or developmental pathways may therefore disrupt sex-specific allocation strategies, leading to contraction, exaggeration or reversal of dimorphism (Klein, 2004). While sex-biased effects of parasitism are well documented for survival and reproduction (Zuk & McKean, 1996; Shine, 1989), our results extend these patterns to structural morphology itself, demonstrating that parasites can reshape the physical expression of sexual phenotypes.

Cross-system convergence: parallels with rhizocephalan-induced feminization

The morphological restructuring observed here closely parallels patterns reported in rhizocephalan–crab systems, where parasites induce feminization, loss of male secondary sexual traits and reallocation of growth toward female-like structures (Reinhard, 1956; Høeg,

1995). Quantitative analyses show that infected male crabs shift along existing allometric trajectories toward female trait proportions rather than undergoing uniform shrinkage, mirroring the proportional changes detected in mantids (Toyota et al., 2023; Kajimoto et al., 2025). Despite the deep phylogenetic distance between insects infected by horsehair worms and crustaceans infected by rhizocephalans, both systems exhibit convergent reorganization of trait allocation. This convergence suggests that parasites can act as developmental engineers, redirecting host growth through interference with conserved regulatory pathways (Høeg, 1995; Lafferty & Shaw 2013).

Parasites as drivers of phenotypic and evolutionary diversification

By modifying allometric relationships, parasites alter locomotor performance, reproductive potential and survival, thereby reshaping selective landscapes experienced by hosts. Recurrent parasite-mediated reallocation of trait investment may constrain or redirect the evolution of sexually dimorphic and performance-related traits over evolutionary timescales (Violle et al., 2007). While parasite-driven selection is already recognized as a powerful force shaping behavior and life histories (Sato et al., 2012; Lafferty & Shaw, 2013), our results demonstrate that it also operates directly on body-plan architecture. Integrating parasitism into trait-based ecology is therefore essential for understanding how organismal form, function and evolutionary diversification are linked (Violle et al., 2007).

Conclusions

Horsehair worm infection reshapes mantis morphology by modifying proportional investment among traits, producing sex-specific and species-specific changes in functional architecture. Similar restructuring in rhizocephalan–crab systems indicates that parasite-driven modification of host trait allocation may represent a general ecological phenomenon across taxa. Integrating parasitism into trait-based ecology is therefore essential for understanding how organismal form, performance and evolution are linked.

References

Brannoch, S. K., Wieland, F., Rivera, J., Klass, K. D., Béthoux, O., & Svenson, G. J. (2017). Manual of praying mantis morphology, nomenclature, and practices (Insecta, Mantodea). *ZooKeys*, 696, 1–100.

Chiu, M. C., Huang, C. G., Wu, W. J., & Shiao, S. F. (2015). Morphological allometry and intersexuality in horsehair-worm-infected mantids, *Hierodula formosana* (Mantodea: Mantidae). *Parasitology*, 142, 1130–1142.

Folmer, O., Black, M., Hoeh, W., Lutz, R. & Vrijenhoek R. (1994). DNA primers for amplification of mitochondrial cytochrome c oxidase subunit I from diverse metazoan invertebrates. *Molecular Marine Biology and Biotechnology*, 3, 294–297.

Hatcher, M. J., Dick, J. T. A. & Dunn, A. M. (2012). Diverse effects of parasites in ecosystems: linking interdependent processes. *Frontiers in Ecology and the Environment*, 10, 186–194.

Høeg, J. T. (1995). The biology and life cycle of the Rhizocephala (Cirripedia). *Journal of the Marine Biological Association of the United Kingdom*, 75, 517–550. doi:10.1017/S0025315400038996

Kajimoto, A., Iwasaki, A., Ohira, T., & Toyota, K. (2025). Morphological feminization in hermit crabs (family Paguridae) induced by rhizocephalan barnacles. *Zoological letters*, 11(1), 6.

Klein S. L. (2004). Hormonal and immunological mechanisms mediating sex differences in parasite infection. *Parasite Immunology*, 26, 247–264.

Lafferty, K. D., & Shaw, J. C. (2013). Comparing mechanisms of host manipulation across host and parasite taxa. *The Journal of Experimental Biology*, 216, 56–66.

Mishina, T., Chiu, M. C., Hashiguchi, Y., Oishi, S., Sasaki, A., Okada, R., Uchiyama, H., Sasaki, T., Sakura, M., Takeshima, H., & Sato, T. (2023). Massive horizontal gene transfer and the evolution of nematomorph-driven behavioral manipulation of mantids. *Current Biology*, 33, 4988–4994.

Nakamine, H., Explanation; Mantodea, in: Machida R. (Ed.), The Standard of polyneoptera in Japan, Gakken Plus Co. Ltd., Tokyo, 2016, pp. 198–205 (in Japanese).

Obayashi, N., Iwatani, Y., Sakura, M., Tamotsu, S., Chiu, M. C., & Sato, T. (2021). Enhanced polarotaxis can explain water-entry behaviour of mantids infected with nematomorph parasites. *Current Biology*, 31(12), R777–R778.

Poulin, R. (2010). Parasite manipulation of host behavior: An update and frequently asked questions. *Advances in the Study of Behavior*, 41, 151–186.

Reinhard, E. G. (1956). Parasitic castration of crustacea. *Experimental parasitology*, 5, 79–107.

R Core Team (2025). R: A language and environment for statistical computing. R Foundation for Statistical Computing, Vienna, Austria. https://www.R-project.org/.

Sato, T., Egusa, T., Fukushima, K., Oda, T., Ohte, N., Tokuchi, N., Watanabe, K., Kanaiwa, M., Murakami, I., & Lafferty, K. D. (2012). Nematomorph parasites indirectly alter the food web and ecosystem function of streams through behavioural manipulation of their cricket hosts. *Ecology Letters*, 15, 786–793.

Sato, T., Watanabe, K., Kanaiwa, M., Niizuma, Y., Harada, Y., & Lafferty, K. D. (2011). Nematomorph parasites drive energy flow through a riparian ecosystem. *Ecology*, 92, 201–207.

Sawada, Y., Sato, N., Osawa, T., Matsumoto, K., Chiu, M. C., Okada, R., Sakura, M., & Sato, T. (2024). A potential evolutionary trap for the extended phenotype of a nematomorph parasite. *PNAS nexus*, 3, 464.

Shine R. (1989). Ecological causes for the evolution of sexual dimorphism: a review of the evidence. *The Quarterly Review of Biology*, 64, 419–461.

Stecher, G., Tamura, K. & Kumar S. (2020). Molecular evolutionary genetics analysis (MEGA) for macOS. *Molecular Biology and Evolution*, 37, 1237–1239.

Tani, S., Tettey, P. A., Maruta, R., Kodama, A., Saito, H., & Kawai, K. (2024). Host range differences between two species of freshwater horsehair worm (Nematomorpha: Chordiidae) *Chordodes japonensis* and *C. formosanus* in Japan. *Parasitology international*, 99, 102847.

Thomas, F., Schmidt-Rhaesa, A., Martin, G., Manu, C., Durand, P. & Renaud, F. (2002), Do hairworms (Nematomorpha) manipulate the water seeking behaviour of their terrestrial hosts? *Journal of Evolutionary Biology*, 15, 356-361.

Toyota, K., Ito, T., Morishima, K., Hanazaki, R., & Ohira, T. (2023). *Sacculina*-induced morphological feminization in the grapsid crab *Pachygrapsus crassipes*. *Zoological Science*, 40, 367–374.

Violle, C., Navas, M.L., Vile, D., Kazakou, E., Fortunel, C., Hummel, I. & Garnier, E. (2007), Let the concept of trait be functional! *Oikos*, 116, 882–892.

West, G. B., Brown, J. H., & Enquist, B. J. (1997). A general model for the origin of allometric scaling laws in biology. *Science*, 276, 122–126.

Zuk, M., & McKean, K. A. (1996). Sex differences in parasite infections: patterns and processes. *International Journal for Parasitology*, 26, 1009–1023.

Figures with legends

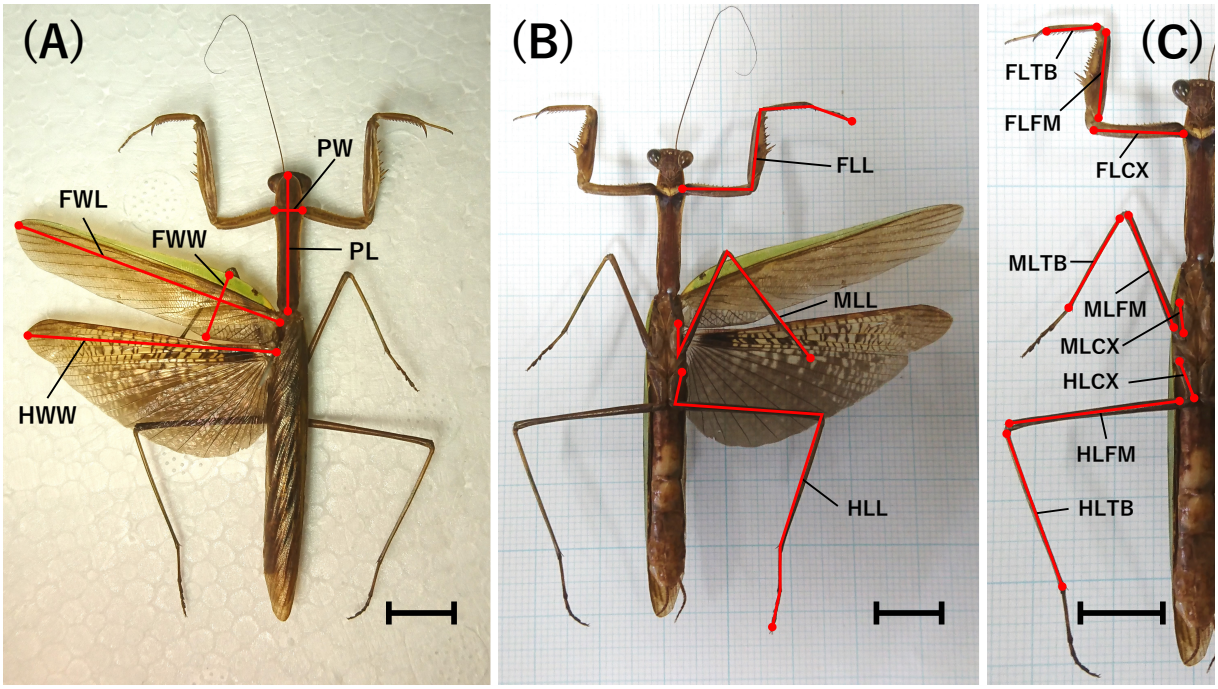

Figure 1. Appearance of the body parts of praying mantises that were the subject of morphological measurements

(A) dorsal view, (B) ventral view, (C) enlarged ventral view of a *T. sinensis* specimen. The scale bar on each photo represents 1 cm. PL: pronotum length, PW: pronotum width, FWL: forewing length, FWW: forewing width, HWL: hindwing length, FLL: length of fore-leg, FLCX: length of fore-coxa, FLFM: length of fore-femur, FLTB: length of fore-tibia, MLL: lengths of mid-leg, MLCX: length of mid-coxa, MLFM: length of mid-femur, MLTB: length of mid-tibia, HLL: lengths of hind-leg, HLCX: length of hind-coxa, HLFM: length of hind-femur and HLTB: length of hind-tibia.

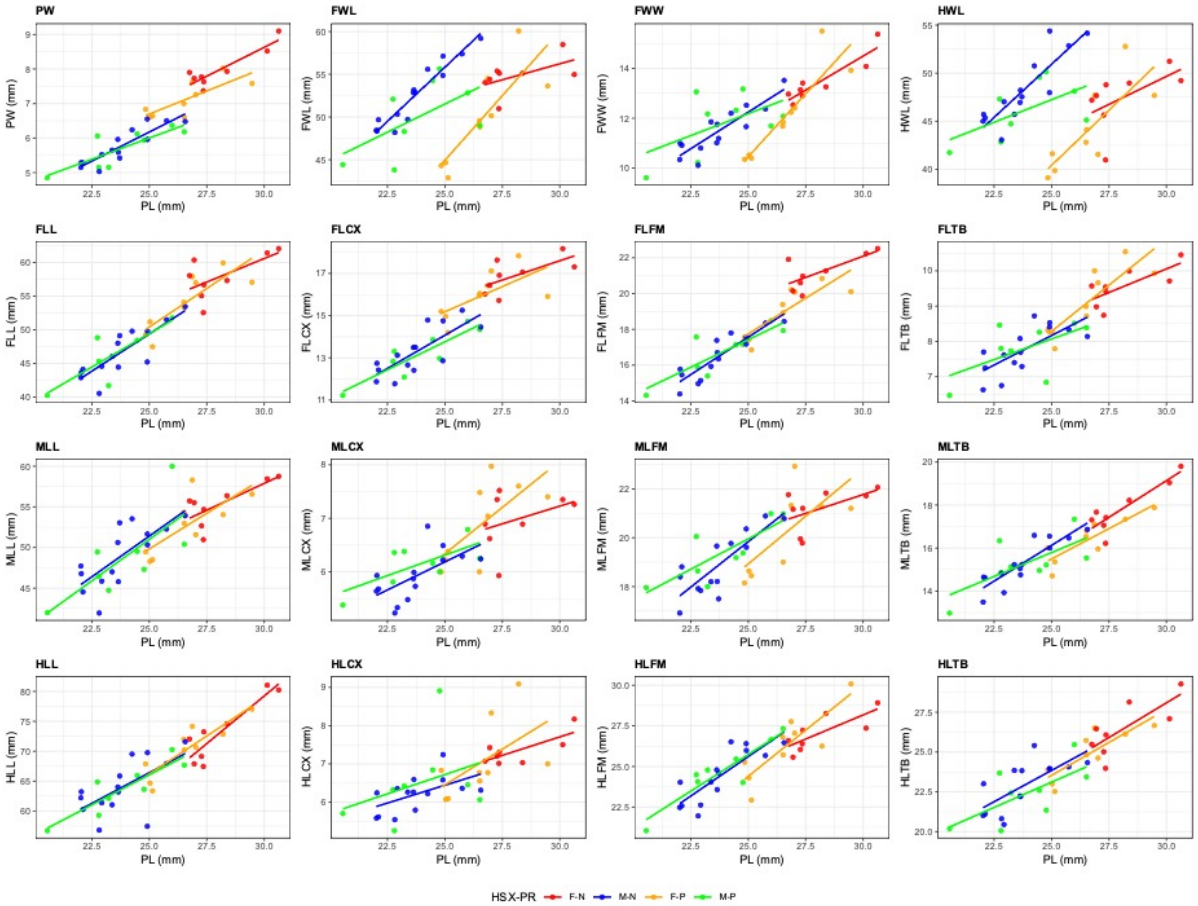

Figure 2. Trait–size relationships for *Tenodera sinensis* morphology.

Scatterplots show scaling relationships between pronotum length (PL; body size proxy) and representative morphological traits for *T. sinensis*. Points represent individuals and colors indicate sex × parasite groups (female–uninfected, male–uninfected, female–infected, male–infected). Lines show fitted linear regressions for each group. Differences in slopes or intercepts indicate parasite- and sex-specific changes in allometric allocation. Divergence among regression lines reflects shifts in proportional investment among traits rather than uniform changes in body size.

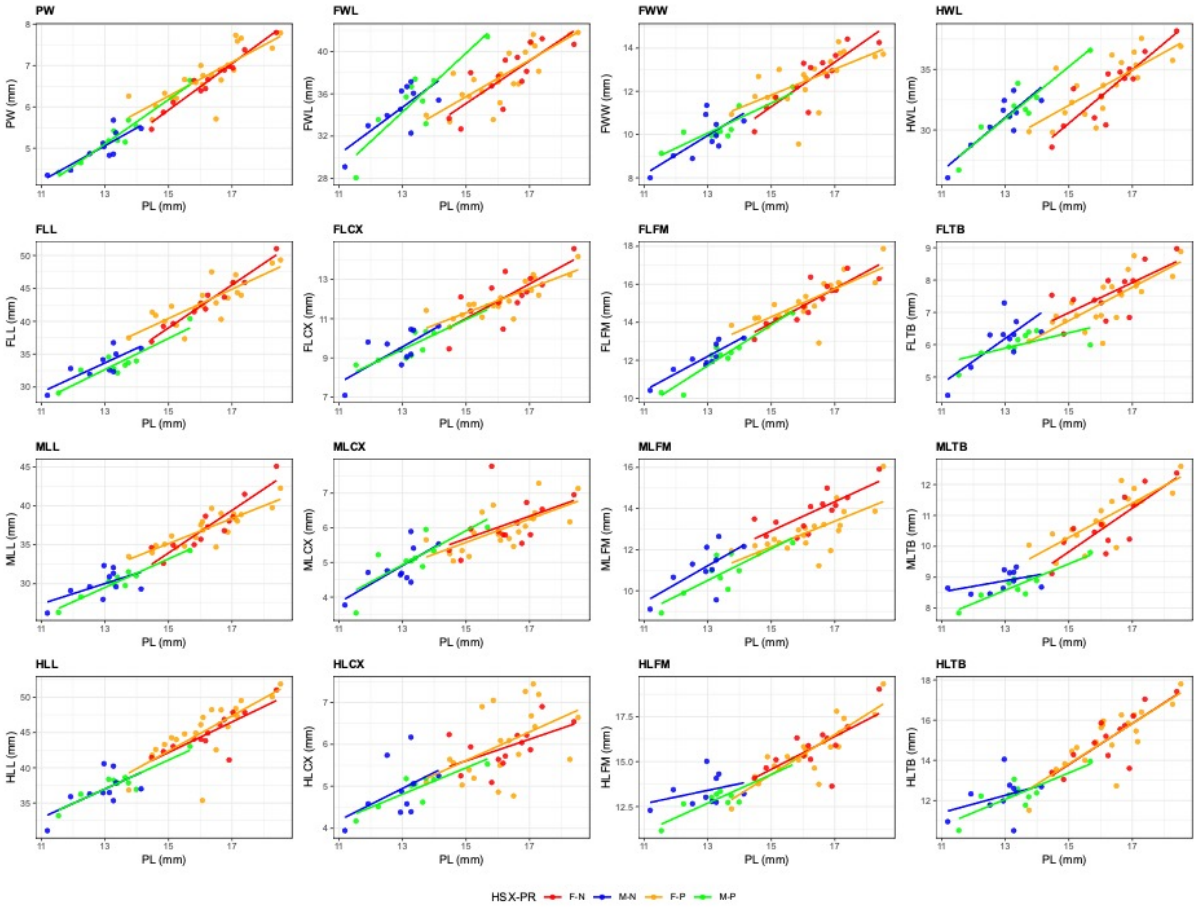

Figure 3. Trait–size relationships for *Hierodula patellifera* morphology.

Scatterplots show scaling relationships between PL and representative morphological traits for *H. patellifera*. Points represent individuals and colors indicate sex × parasite groups (female–uninfected, male–uninfected, female–infected, male–infected). Lines show fitted linear regressions for each group. Differences in slopes or intercepts indicate parasite- and sex-specific changes in allometric allocation. Divergence among regression lines reflects shifts in proportional investment among traits rather than uniform changes in body size.

463 **Tables**

464 **Table 1. ANCOVA results for allometric relationships in *Tenodera sinensis*.**

465 Estimates (± SE) for parasite status (PR), host sex (HSX), their interaction (PR × HSX), and
466 body size (PL) effects on each morphological trait. Significance codes: 0 '***' 0.001 '**' 0.01
467 '*' 0.05 '.' 0.1.

Trait	PR (Estimate ± SE)	HSX (Estimate ± SE)	PR × HSX (Estimate ± SE)	PL	R2
PW	− 0.06668 ± 0.12699	**0.96984 ± 0.18394*** **	**− 0.35347 ± 0.19329.**	***	0.93
FWL	**− 2.8828 ± 1.2306***	**− 6.2273 ± 1.7824****	0.9431 ± 1.8730	***	0.59
FWW	0.20034 ± 0.34263	− 0.66043 ± 0.49627	− 0.67329 ± 0.52151	***	0.68
HWL	**− 2.1958 ± 1.1321.**	**− 7.7314 ± 1.6398*****	1.5497 ± 1.7232	***	0.54
FLCX	− 0.18845 ± 0.31292	**1.34638 ± 0.45324****	− 0.02555 ± 0.47629	***	0.86
FLFM	0.12347 ± 0.31536	**1.67479 ± 0.45677*****	**− 1.19143 ± 0.47999***	***	0.90
FLTB	0.01396 ± 0.22807	0.34894 ± 0.33033	0.06065 ± 0.34713	***	0.76
MLCX	0.18797 ± 0.20563	0.09561 ± 0.29783	− 0.03335 ± 0.31297	***	0.57
MLFM	0.40553 ± 0.39453	− 0.32132 ± 0.57143	− 0.49516 ± 0.60049	***	0.65
MLTB	− 0.07624 ± 0.28215	0.06989 ± 0.40867	− 0.44304 ± 0.42946	***	0.81
HLCX	0.25617 ± 0.28719	0.12379 ± 0.41596	− 0.28006 ± 0.43711	**	0.39
HLFM	0.2128 ± 0.4155	**− 1.3097 ± 0.6018***	0.3973 ± 0.6324	***	0.77
HLTB	− 0.5672 ± 0.4974	0.2475 ± 0.7205	0.1322 ± 0.7571	***	0.74

468

469

Table 2. ANCOVA results for allometric relationships in *Hierodula patellifera*.

Estimates (± SE) for parasite status (PR), host sex (HSX), their interaction (PR × HSX), and body size (PL) effects on each morphological trait. Significance codes: 0 '***' 0.001 '**' 0.01 '*' 0.05 '.' 0.1.

Trait	PR (Estimate ± SE)	HSX (Estimate ± SE)	PR × HSX (Estimate ± SE)	PL	R2
PW	0.06133 ± 0.13637	0.03183 ± 0.17933	0.09426 ± 0.17336	***	0.91
FWL	− 0.1228 ± 0.8059	**− 3.7606 ± 1.0598*** **	0.5211 ± 1.0245	***	0.68
FWW	0.10870 ± 0.36501	0.19899 ± 0.47998	− 0.06809 ± 0.46400	***	0.77
HWL	0.0970 ± 0.6571	**− 3.6323 ± 0.8641*** **	0.5362 ± 0.8353	***	0.72
FLCX	− 0.10333 ± 0.30565	0.22254 ± 0.40193	0.02380 ± 0.38855	***	0.83
FLFM	− 0.39231 ± 0.28018	0.14232 ± 0.36844	0.50154 ± 0.35617	***	0.89
FLTB	− 0.36726 ± 0.24239	− 0.12686 ± 0.31874	0.17244 ± 0.30813	***	0.72
MLCX	0.08346 ± 0.23705	− 0.03617 ± 0.31172	− 0.17464 ± 0.30135	***	0.62
MLFM	**− 0.65749 ± 0.34160.**	0.33244 ± 0.44921	− 0.20553 ± 0.43425	***	0.77
MLTB	**− 0.39530 ± 0.21818.**	0.05040 ± 0.28691	**0.66686 ± 0.27736***	***	0.86
HLCX	− 0.13095 ± 0.27657	− 0.06952 ± 0.36370	0.25698 ± 0.35159	***	0.50
HLFM	**− 0.8438 ± 0.3957***	− 0.8378 ± 0.5204	0.8231 ± 0.5031	***	0.77
HLTB	− 0.3533 ± 0.3949	− 0.1500 ± 0.5193	0.3597 ± 0.5020	***	0.79

476 **Table 3. Estimated marginal means (EMM) contrasts for sexual dimorphism and parasite**
477 **effects in *Tenodera sinensis*.**

478 Values represent pairwise differences ± SE between groups at mean body size. F = female, M
479 = male, N = uninfected, P = infected. Significance codes: 0 '***' 0.001 '**' 0.01 '*' 0.05 '.' 0.1.

Trait	Sex difference (Non-para.) (F−M)	Parasite effect (Male) (P−N)	Parasite effect (Female) (P−N)	Sex difference (Para.) (F−M)
PW	**0.970 ± 0.184*** **	− 0.0667 ± 0.127	**− 0.4201 ± 0.144** **	**0.616 ± 0.158*** **
FWL	**− 6.23 ± 1.78** **	**− 2.88 ± 1.23***	− 1.94 ± 1.40	**− 5.28 ± 1.53** **
FWW	− 0.66 ± 0.496	0.200 ± 0.343	− 0.473 ± 0.390	**− 1.33 ± 0.426** **
HWL	**− 7.73 ± 1.64*** **	**− 2.196 ± 1.13.**	− 0.646 ± 1.29	**− 6.18 ± 1.41*** **
FLCX	**1.35 ± 0.453** **	− 0.188 ± 0.313	− 0.214 ± 0.356	**1.32 ± 0.389** **
FLFM	**1.675 ± 0.457*** **	0.123 ± 0.315	**− 1.068 ± 0.359** **	0.483 ± 0.392
FLTB	0.349 ± 0.330	0.0140 ± 0.228	0.0746 ± 0.259	0.410 ± 0.283
MLCX	0.0956 ± 0.298	0.188 ± 0.206	0.155 ± 0.234	0.0623 ± 0.256
MLFM	− 0.321 ± 0.571	0.4055 ± 0.395	− 0.0896 ± 0.449	− 0.816 ± 0.490
MLTB	0.0699 ± 0.409	− 0.0762 ± 0.282	− 0.5193 ± 0.321	− 0.3731 ± 0.351
HLCX	0.124 ± 0.416	0.2562 ± 0.287	− 0.0239 ± 0.327	− 0.156 ± 0.357
HLFM	**− 1.310 ± 0.602***	0.213 ± 0.415	0.610 ± 0.473	**− 0.912 ± 0.516.**
HLTB	0.248 ± 0.720	− 0.567 ± 0.497	− 0.435 ± 0.566	0.380 ± 0.618

480

481

Table 4. Estimated marginal means (EMM) contrasts for sexual dimorphism and parasite effects in *Hierodula patellifera*.

Values represent pairwise differences ± SE between groups at mean body size. F = female, M = male, N = uninfected, P = infected. Significance codes: 0 '***' 0.001 '**' 0.01 '*' 0.05 '.' 0.1.

Trait	Sex difference (Non-para.) (F−M)	Parasite effect (Male) (P−N)	Parasite effect (Female) (P−N)	Sex difference (Para.) (F−M)
PW	0.0318 ± 0.179	0.0613 ± 0.136	0.1556 ± 0.106	0.1261 ± 0.157
FWL	**−3.76 ± 1.060*** **	−0.123 ± 0.806	0.398 ± 0.628	**−3.24 ± 0.925** **
FWW	0.199 ± 0.480	0.1087 ± 0.365	0.0406 ± 0.285	0.131 ± 0.419
HWL	**−3.63 ± 0.864*** **	0.097 ± 0.657	0.633 ± 0.512	**−3.10 ± 0.754*** **
FLCX	0.223 ± 0.402	−0.1033 ± 0.306	−0.0795 ± 0.238	0.246 ± 0.351
FLFM	0.142 ± 0.368	−0.392 ± 0.280	0.109 ± 0.218	**0.644 ± 0.322.**
FLTB	−0.1269 ± 0.319	−0.367 ± 0.242	−0.195 ± 0.189	0.0456 ± 0.278
MLCX	−0.0362 ± 0.312	0.0835 ± 0.237	−0.0912 ± 0.185	−0.2108 ± 0.272
MLFM	0.332 ± 0.449	**−0.657 ± 0.342.**	**−0.863 ± 0.266** **	0.127 ± 0.392
MLTB	0.0504 ± 0.287	**−0.395 ± 0.218.**	0.272 ± 0.170	**0.7173 ± 0.250** **
HLCX	−0.0695 ± 0.364	−0.131 ± 0.277	0.126 ± 0.216	0.1875 ± 0.317
HLFM	−0.8378 ± 0.520	**−0.8438 ± 0.396***	−0.0207 ± 0.308	−0.0148 ± 0.454
HLTB	−0.15 ± 0.519	−0.35329 ± 0.395	0.00645 ± 0.308	0.21 ± 0.453